J. Biochem. 125, 48-57 (1999)

Primary Structure, Expression, and Site-Directed Mutagenesis of Inorganic Pyrophosphatase from *Bacillus stearothermophilus*[1]

Takanori Satoh,* Hiroshi Shinoda,* Keisuke Ishii,*,[2] Masayuki Koyama,* Nobuhiko Sakurai,*,[3] Hiroyuki Kaji,*,[4] Akira Hachimori,† Masachika Irie,‡ and Tatsuya Samejima*,[5]

**Department of Chemistry, College of Science and Engineering, Aoyama Gakuin University, Chitosedai, Setagaya-ku, Tokyo 157-8572; †Institute of High Polymer Research, Faculty of Textile Science and Technology, Shinshu University, Ueda, Nagano 386-8567; and ‡Department of Microbiology, Hoshi College of Pharmacy, Ebara, Shinagawa-ku, Tokyo 142-0063*

Received July 14, 1998; accepted September 28, 1998

The complete primary structure of inorganic pyrophosphatase [EC 3.6.1.1] from *Bacillus stearothermophilus* (ATCC 12016) was determined at the amino acid level by automated Edman degradation. The subunit of the enzyme consists of 164 amino acid residues with a calculated molecular mass of 18,796. The amino acid sequence of the enzyme is almost identical to that of thermophilic bacterium PS-3. Based on the determined primary structure, a PCR-amplified semi-synthetic gene was constructed and expressed in *Escherichia coli* JM109. The recombinant *Bst.* PPase showed the same characteristics and activity as the authentic enzyme, and exhibits higher thermostability than the *E. coli* enzyme. Furthermore, we prepared tyrosine-substituted variants by site-directed mutagenesis to elucidate the role of two highly conserved tyrosines (Y46 and Y130). As a result, two variants, Y46F and Y130F, lost most of their enzyme activity, whereas their conformations were unaffected. However, the wild-type and two variants exhibited different thermostability behaviors in the presence or absence of Mg^{2+}. Therefore, these tyrosines may contribute to the structural integrity of the active site of the enzyme.

Key words: amino acid sequence, *Bacillus stearothermophilus*, expression, inorganic pyrophosphatase, site-directed mutagenesis.

Inorganic pyrophosphatase (PPase, pyrophosphate phosphohydrolase) [EC 3.6.1.1] hydrolyzes inorganic pyrophosphate to two orthophosphates to maintain biosynthetic equilibrium for reactions such as DNA synthesis that generate inorganic pyrophosphate (*1*). PPase requires divalent cations such as Mg^{2+}, which are essential for enzyme activity and thermostability (*2*). Some PPases have been isolated from various procaryotes (*3, 4*), eucaryotes (*5, 6*), and archaebacteria (*7, 8*). In eucaryotes, the primary structure has been directly determined by sequencing PPase from *Saccharomyces cerevisiae*, consisting of 286 amino acid residues (Y-PPase) (*9*), and also deduced from the nucleotide sequence of the genes from *Kluyveromyces lactis* (*10*), *Schizosaccharomyces pombe* (*11*), *Arabidopsis thaliana* (*12*), and bovine retina (*13*). In particular, the Y-PPase gene has been cloned (*14, 15*) and expressed in *Escherichia coli* by the pET expression system (*16*). In addition, Y-PPase has been crystallized and its three-dimensional structure determined by X-ray diffraction analysis at 2.2 and 2.0 Å, in which the active center was identified (*17*). In procaryotes, the genes for PPases from *E. coli* (*18*), thermophilic bacterium PS-3 (*19*), and *Thermus thermophilus* HB8 (*Tth.*) (*20*) have been cloned and the primary structure predicted. Also, the amino acid sequence has been determined directly for the *Tth.* (*20*) and PS-3 enzymes (*21*). In addition, the analysis of the three-dimensional structure has been performed on *E. coli* PPase at 1.9 Å (*22*) and *Tth.* PPase at 2.0 Å (*23*). The three-dimensional structures of both enzymes are very similar but they differ in their oligomeric interactions. In this respect, it has been deduced that the *Tth.* PPase acquires stability by oligomerization, thereby inducing many additional hydrogen bonds and ionic interactions (*24*). Meanwhile, the primary structure of PPases from archaebacteria, *Sulfolobus acidocaldarius* (*25*) and *Thermoplasma acidophilum* (*26*), have been reported. This information will provide some insight as to the mechanisms of thermostability of thermophilic PPases. On the other

[1] This study was partly supported by a grant from the Research Institute of Aoyama Gakuin University. The amino acid sequence reported in this paper has been submitted to the JIPID database with the accession number JH0271. The nucleotide sequence reported in this paper has been submitted to the DDBJ, Gene Bank, and EMBL databases with the accession number AB003087.

Present addresses: [2] Department of Development, Shino-Test Co., Oonodai, Sagamihara, Kanagawa 229-0011; [3] Division of Life Sciences, Graduate School of Natural Science and Technology, Kanazawa University, Kakumamachi, Kanazawa, Ishikawa 920-11; [4] Department of Chemistry, Faculty of Science, Tokyo Metropolitan University, Minami-osawa, Hachioji, Tokyo 192-0364.

[5] To whom correspondence should be addressed. Tel: +81-3-5384-1111 (Ext. 3204), Fax: +81-3-5384-6200, E-mail: samejima@candy.chem.aoyama.ac.jp

Abbreviations: PPase, inorganic pyrophosphatase; *Bst.*, *Bacillus stearothermophilus;* API, *Achromobacter* Protease I; *Tth.*, *Thermus thermophilus* HB8; Y, *Saccharomyces cerevisiae*.

hand, the putative active site residues are highly conserved among the PPases described above. From studies on the three-dimensional structures and site-directed mutagenesis, the active-site residues of some PPases have been determined (*17, 22, 27-29*). Tyrosines, lysines, and so on are included in the active-site cavity, and many interaction networks are formed (*30-32*). Sometimes such interactions can stabilize the structure not only of the active-site, but also of the whole molecule (*30*).

Inorganic pyrophosphatase from *Bacillus stearothermophilus* (*Bst.* PPase) is also a procaryotic PPase, and some of its characteristics have been reported previously (*33*). However, little information exists about the structures, *e.g.* the primary, active-site, and three-dimensional structures. In order to understand the thermostabilization, it is crucial to investigate the structure and function of this thermophilic PPase. Therefore, in this report we describe the complete primary structure, expression of the semi-synthetic gene, characterization of the recombinant protein expressed in *E. coli* cells, and contribution of the conserved tyrosines to the enzyme activity and thermostability of thermophilic *Bst.* PPase.

MATERIALS AND METHODS

Organisms—*B. stearothermophilus* ATCC12016 was grown aerobically at 65°C in a medium described previously (*33*). The mass cultures were kindly supplied by the Central Research Laboratories, Ajinomoto.

Preparation of Authentic B. stearothermophilus (Bst.) PPase—The enzyme was purified from *Bst.* cell extracts by the method of Hachimori *et al.* as reported previously (*33*) with slight modifications. Briefly, the crude extract prepared by sonication and deoxyribonuclease digestion was heated under conditions resulting in no loss of enzyme activity (80°C, 15 s), and the resultant supernatant was concentrated by ammonium sulfate precipitation (60-90% sat.). The protein solution with PPase activity was then subjected to DEAE-Cellulose (DE-52, Whatman) column chromatography followed by Sephacryl S-200 HR (Pharmacia) gel chromatography. If necessary, HPLC on an ion-exchange column was performed until the enzyme showed a single band on polyacrylamide gel electrophoresis. Purification of recombinant *Bst.* PPase followed almost the same procedure, except for the heat treatment and ammonium sulfate precipitation.

Preparation of Recombinant E. coli PPase—*E. coli* PPase gene was cloned and expressed in *E. coli* JM109 according to Lahti *et al.* as reported previously (*18*). However, we found that our cloned *E. coli* PPase contains Ser22 instead of Pro22 as reported for PPase from *E. coli* K-12 strain (*18*). The reason for this discrepancy is not clear at present. Purification was performed by the same method as described above.

Protease Digestion and Protein Sequencing—For the sequencing, the isolated enzyme was first denatured, reduced, and *S*-pyridylethylated. Then, the enzyme was cleaved into fragments by enzymatic digestions with *Staphylococcus aureus* V8 protease (Worthington), *Achromobacter* protease I (Lysyl endopeptidase, Wako Pure Chemicals), and trypsin (Wako Pure Chemicals), and subjected to chemical cleavage with a formic acid-pyridine solution (pH 2.5). Peptide fragments were obtained by reverse phase HPLC on a Biofine RPC-SC18 column (Jasco). The amino acid sequence was determined by automated Edman degradation using Protein Sequencers from Applied Biosystems (model 477A) and Shimadzu PSQ-1. The carboxyl-terminal residue was determined by carboxypeptidase P digestion followed by amino acid composition analysis.

Preparation of Genomic DNA from Bst.—The *Bst.* genomic DNA used as a template for the polymerase chain reaction (PCR) was prepared with the method of Saito and Miura (*34*). Bacterial cells were lysed with lysozyme in 150 mM NaCl/100 mM EDTA and then by repeated freeze and thaw. The DNA was extracted 5 times with phenol saturated with TE buffer (10 mM Tris-HCl, 1 mM EDTA, pH 8) and treated with ribonuclease A. Finally, the DNA was collected by ethanol precipitation.

Oligonucleotides Synthesis—Oligonucleotide primers for PCR and linker DNA were designed by the optimal codon usage for *E. coli* according to the amino acid sequence of *Bst.* PPase determined by the above method. The primers were obtained commercially from Biologica. The sense-primer for PCR corresponding to Phe2-Val7 was 5′-TT(T/C)GA(A/G)AA(T/C)AA(A/G)AT(T/C/A)GT-3′ (17mer) and the antisense-primer to Ala158-Lys164 with a stop codon was 5′-GCA AGC TTC AAG CTT ATC ATT TTT GTT CGT TAT AGC GGG-3′ (39mer). Linker DNA oligomers for construction of the expression vector pMK2PPAQ were 5′-GAT AAG CTT GAA TTC ATG GCC-3′ (21mer) (Initiation Met and Ala1) and 5′-GGC CAT GAA TTC AAG CTT ATC-3′ (21mer).

Site-Directed Mutagenesis by Polymerase Chain Reaction—Site-directed mutagenesis was performed by the polymerase chain reaction. All variants were constructed by a recombinant PCR method. All variant DNA fragments described below were amplified by a common sense-primer 5′-GAT GCG TCC GGC GTA GAG GAT-3′ [21mer, corresponding to the sequence in pMK2 vector (*35*)], and a common antisense-primer 5′-CCG CGG ATT TGT CCT ACT C-3′ (19mer, complementary to the sequence in pMK2 vector). For Y130F, the upper fragment was amplified by a sense-primer and 5′-CCT TGC AGA TCT TTA AAC CGT TCA AA-3′ (26mer, complementary to Phe127-Gly135), while the lower fragment was amplified by an antisense-primer and 5′-GAG CGG TTT AAA GAT CTA CAA GG-3′ (23mer, corresponding to Glu128-Gly135). These upper and lower fragments amplified by the first PCR were denatured and annealed, followed by the second PCR using sense- and antisense primers. The PCR products for all variant mutations were digested with *Bam*HI-*Nsi*I, and the resulting fragment was inserted into the corresponding position of an original vector, pMK2PPAQ. In the case of Y46F, the upper fragment was amplified by a sense-primer and 5′-ATA GCC AAA TTC CGC GGG ATA-3′ (21mer, complementary to Tyr42-Tyr48), and the lower fragment was amplified by an antisense-primer and 5′-ATG TTC TTT CCC GCG GAG TTC-3′ (27mer, corresponding to Met40-Tyr46); this primer was also used for Y42F variants (unpublished data). Using these upper and lower fragments, the Y46F vector was constructed by the same procedure as for Y130F.

DNA Sequencing—DNA sequencing was performed by the dideoxy chain termination method using a Sequenase ver. 2 sequencing kit (TOYOBO) and a *Bca* BEST dideoxy

sequencing kit (Takara Shuzo) with a Hitachi SQ-3000 fluorescence DNA sequencer.

Enzyme Assay—The activity of PPase was assayed at 37°C according to a previously described procedure (*33*) in which the liberation of inorganic phosphate was determined by the method of Peel and Loughman (*36*). Protein concentrations were determined by the method of Lowry *et al.* (*37*) using bovine serum albumin as a standard.

Circular Dichroism (CD) Measurements—CD spectra were obtained with a JASCO J-600 automatic recording dichrograph at room temperature. The protein concentration of each sample was 0.1 mg/ml. Cells with a 1 mm pathlength were used for measurements in the far-ultraviolet region. CD data are expressed in terms of mean residue ellipticity [θ] using a mean residue molecular weight from the determined primary structure.

Fluorescence Measurements—Fluorescence measurements were made using a JASCO FP777 spectrofluorometer at room temperature. The protein concentration was always adjusted to 0.05 mg/ml in 20 mM Tris-HCl buffer (pH 7.8). Tyrosine excitation was at 275 nm, tryptophan excitation was at 295 nm. The emission spectra were set between 300 and 400 nm.

RESULTS

Primary Structure of PPase from Bst.—The primary structure of *Bst.* PPase was determined by conventional fragmentation followed by automated Edman degradation. The sequence of the enzyme was aligned by overlapping the sequence of each fragment by at least two residues. At first, 27 residues of the N-terminal region were sequenced in the *S*-pyridylethylated protein. Twenty-three peaks were separated from the V8 protease digest by reverse-phase HPLC, and most were subjected to sequence analysis. We could detect all amino acid residues except for residue nos. 92, 103-113, 123-128, and 163-164 in the V8 protease digestion products (Fig. 1). Then, we obtained 12 peptides from the API digest by HPLC and determined the sequences of four of the peptide fragments. Tryptic digestion yielded 37 peaks by HPLC and ten of the peptide fragments were sequenced. The chemical scission of Asp-Pro by formic acid yielded three peptides as expected, and all were partially sequenced from their N-termini. The C-terminal residue, Lys, was determined by treatment with carboxypeptidase P. Thus, the complete amino acid sequence of *Bst.* PPase was aligned by overlapping the sequences of the examined peptide fragments. Figure 1 shows the determined amino acid sequence comprising 164 residues with a calculated molecular mass of 18,796. No post-translational modifications were detected. The sequence was almost identical to that of thermophilic bacterium PS-3 except for an additional two C-terminal amino acids, Asn-Lys, in the PS-3 enzyme (*19*). However, the sequence of the *Bst.* enzyme is identical to the PS-3 enzyme at the amino acid level except for Pro70 (*21*) which is replaced by Thr70 in the *Bst.* enzyme.

Construction of Expression Vectors for Bst. PPase and

```
1    A  F  E  N  K  I  V  E  A  F  I  E  I  P  T
1       ttt gag aat aag att gtC GAA GCG TTT ATC GAA ATT CCA ACT

16   G  S  Q  N  K  Y  E  F  D  K  E  R  G  I  F
43  GGG AGC CAA AAC AAA TAC GAA TTC GAC AAA GAA CGG GGC ATT TTC

31   K  L  D  R  V  L  Y  S  P  M  F  Y  P  A  E
88  AAG CTC GAC CGC GTC TTA TAT TCA CCG ATG TTT TAT CCG GCT GAA

46   Y  G  Y  L  Q  N  T  L  A  L  D  G  D  P  L
133 TAC GGC TAT TTG CAA AAT ACG TTG GCG CTG GAT GGC GAC CCG CTC

61   D  I  L  V  I  T  T  N  P  T  F  P  G  C  V
178 GAC ATT TTG GTC ATC ACG ACA AAC CCG ACG TTC CCG GGC TGT GTC

76   I  D  T  R  V  I  G  Y  L  N  M  V  D  S  G
223 ATT GAT ACG CGT GTC ATC GGC TAT TTG AAC ATG GTC GAC AGC GGC

91   E  E  D  A  K  L  I  G  V  P  V  E  D  P  R
268 GAA GAA GAT GCG AAA TTG ATC GGC GTT CCG GTC GAA GAT CCG CGC

106  F  D  E  V  R  S  I  E  D  L  P  Q  H  K  L
313 TTT GAC GAA GTT AGA TCG ATT GAA GAT CTC CCG CAG CAC AAA CTG

121  K  E  I  A  H  F  F  E  R  Y  K  D  L  Q  G
358 AAA GAA ATC GCC CAC TTC TTT GAA CGC TAC AAA GAC TTG CAA GGG

136  K  R  T  E  I  G  T  W  E  G  P  E  A  A  A
403 AAA CGG ACG GAA ATC GGC ACA TGG GAG GGG CCG GAA GCA GCC GCC

151  K  L  I  D  E  C  I  A  R  Y  N  E  Q  K    164
448 AAA TTG ATC GAC GAA TGC ATC Gcc cgc tat aac gaa caa aaa   489
```

Fig. 2. **Nucleotide sequence of the gene fragment for the inorganic pyrophosphatase from *Bst.* and its deduced amino acid sequence.** Nucleotides are numbered starting at the second Phe residue (corresponding to TTT) in the primary structure of *Bst.* PPase. The base sequences shown in lowercase letters indicate portions of the PCR primers having degeneracy designed by the amino acid sequence determined preliminarily.

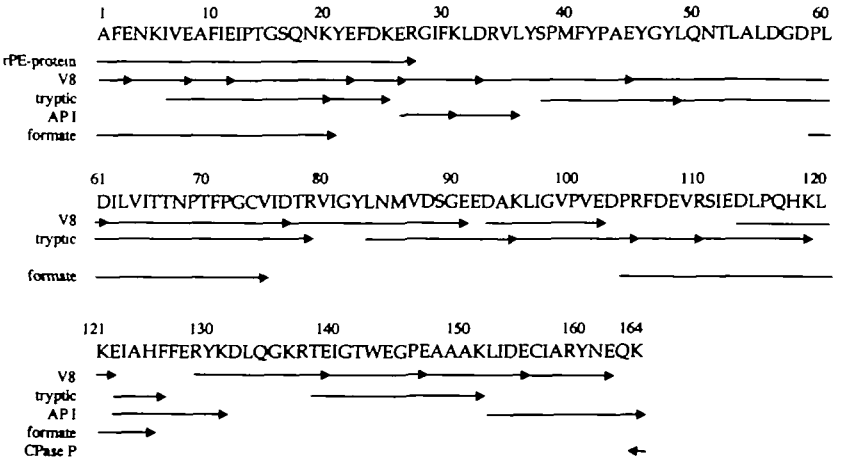

Fig. 1. **The complete amino acid sequence of the inorganic pyrophosphatase (PPase) from *Bacillus stearothermophilus* (*Bst.*).** Amino acid residues are shown by one-letter symbols. Arrows indicate the determined sequence for each peptide obtained by digestion with trypsin (tryptic), *S. aureus* V8 protease (V8), and *Achromobacter* protease I (API), and by chemical cleavage with formate-pyridine (formate). The amino-terminal sequence was determined for the reduced and *S*-pyridylethylated enzyme (rPE-protein). The carboxy-terminal residue was detected by amino acid composition analysis for carboxypeptidase P (CPase P) digest of the full-length protein.

Its Expression in E. coli JM109—The PPase gene was amplified by PCR using primers and *Taq* DNA polymerase with the obtained genomic DNA as a template. The amplified DNA fragment (about 500 bp) was isolated, treated with klenow fragment, ligated into a pUC18 plasmid, and sequenced by the dideoxy chain termination method. The results revealed that the PCR-amplified product contained a coding region for the PPase corresponding to the sequence from Phe2 to the stop codon as designed. We failed to detect any longer fragments in the genomic DNA library. Therefore, we attempted to construct a semi-synthetic gene using the partial gene with the synthetic DNA linker at its 5′-terminus. The resultant semi-synthetic gene was inserted into the *Eco*RI and *Hin*dIII sites of a plasmid vector pMK2 (*35*), a potent *tac* promoter and *rrn* B terminator derived from pKK223-3 (Pharmacia) and pUC18 (Takara), for expression in *E. coli* JM109. The nucleotide sequence of the semi-synthetic gene (490 bp) was determined, and the results are shown in Fig. 2 with the translated amino acid sequence. The amino acid sequence deduced from the nucleotide sequence coincided completely with that determined at the peptide level. The strategy for the construction of the expression vector (pMK2PPAQ) is shown in Fig. 3.

E. coli JM109 transformed with pMK2PPAQ was cultured in LB/Amp broth, and the cell lysate obtained by sonication was examined by SDS-PAGE. As a result, the expression of *Bst.* PPase (19 kDa) was confirmed in the crude extract of *E. coli* JM109/pMK2PPAQ. The expressed enzyme was purified to an electrophoretically homogeneous state as described in "MATERIALS AND METHODS. The yield of purified enzyme was about 20 mg from 6 g wet cells per 1 liter of LB/Amp broth. The result of SDS-PAGE of the purified enzyme revealed an estimated molecular mass for the purified enzyme of 19 kDa, corresponding to that of the authentic enzyme from *Bst.* reported previously (*2*); the subunits were completely homogeneous in both the authentic and recombinant enzymes (data not shown).

Characterization of Recombinant Bst. PPase—The puri-

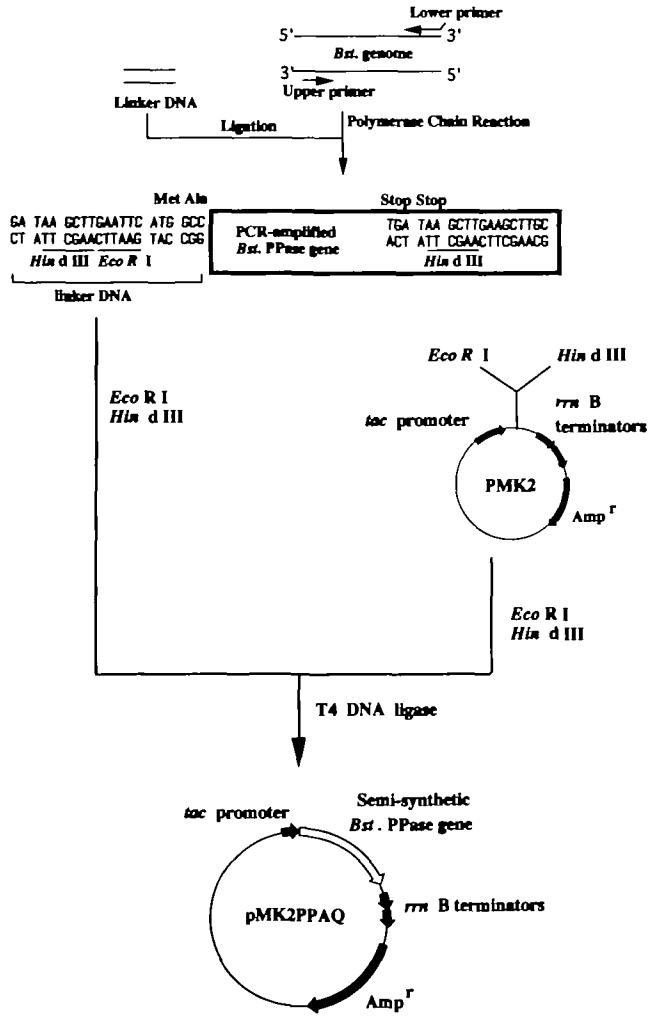

Fig. 3. **Construction of the expression vector, pMK2PPAQ, for the semi-synthetic *Bst.* PPase gene.** Since the DNA fragment amplified by PCR contained additional thymine bases at the 3′-ends, it was treated with klenow fragment to make blunt-end termini. Linker DNA was ligated to this fragment and digested with *Eco*RI and *Hin*dIII. The prepared fragment was introduced into expression vector pMK2 (described in the text) digested with the same restriction endonucleases.

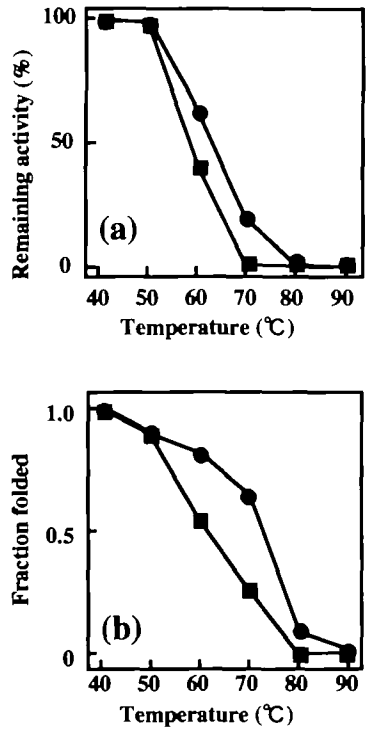

Fig. 4. **Thermostability of recombinant *Bst.* PPase and recombinant *E. coli* PPase.** Panel (a): the remaining activity in both enzymes after heat incubation. The enzyme activity was measured at 37°C and the activity after incubation at 40°C was taken as 100%. Panel (b): conformational changes in both enzymes after incubation. The relative ellipticity of the CD band at 222 nm is plotted against the heating temperature by taking the value at 40°C as unity and at 90°C as zero. The ratio was calculated by the following equation: Fraction folded (ratio of folded protein) = $(Y - Y_D)/(Y_N - Y_D)$, where Y_D and Y_N are the mean residue ellipticities, $[\theta]$, at 222 nm after incubation at 90 and 40°C, respectively, and Y is the measured mean residue ellipticity at the indicated temperatures. In both experiments, the enzyme (0.1 mg/ml) was incubated in Tris-HCl buffer (pH 7.8) at the indicated temperatures for 1 h. Symbols: ●, recombinant *Bst.* PPase; ■, recombinant *E. coli* PPase.

fied recombinant *Bst.* PPase was found to be fully active (about 600 units/mg). The results of amino acid sequencing of the N-terminal five residues without the initial Met residue, the amino acid composition of the whole molecule, and peptide mapping of the API-digest were compared with the data for the authentic enzyme (data not shown). The results showed the recombinant enzyme to be identical to the authentic one. Furthermore, the CD spectrum of the recombinant enzyme was very similar to that of the authentic enzyme, suggesting that the recombinant *Bst.* PPase has the same secondary structure as the authentic enzyme.

Thermostability of Recombinant Bst. PPase—The thermostability of the recombinant *Bst.* PPase was examined and compared to that of recombinant *E. coli* PPase. The recombinant *Bst.* and *E. coli* PPases were incubated in 20 mM Tris-HCl buffer (pH 7.8) at various temperatures for 1 h, and the remaining enzyme activity was measured. The results are shown in Fig. 4a. The *E. coli* enzyme was inactivated completely at 70°C, whereas the *Bst.* enzyme retained about 10% of its activity at the same temperature. To obtain information about changes in the secondary structure of these PPases caused by heating under the same conditions, the relative ellipticity of the CD band at 222 nm was measured. As shown in Fig. 4b, the recombinant *Bst.* PPase was also more thermostable than the *E. coli* enzyme with respect to conformation.

Alignment of the Amino Acid Sequences of PPases from Several Sources—As described above, we confirmed that the recombinant *Bst.* PPase has full enzyme activity and thermostability. However, the residues contributing to the enzyme activity and thermostability of *Bst.* PPase are suggested only by studies involving the chemical modification of His residues (*38*). Therefore, we aligned the amino acid sequence of *Bst.* PPase with those of various PPases, and examined the conserved residues among them. The results are shown in Fig. 5; the relative homology among the amino acid sequences of PPases from several sources is shown in Table I. Although a high homology (above 40%) in primary structure between *Bst.* PPase and procaryotic PPases was observed, the homology between the eucaryotic PPases and *Bst.* PPase was below 40%. As shown in Fig. 5, 22 amino acid residues were highly conserved among all PPases. The X-ray analysis of *Tth.* PPase suggested that 15

TABLE I. **Relative homology of amino acid sequences between *Bst.* and several PPases.**

	Relative homology (%)							
	Sce	*Kla*	*Spo*	*Ath*	*Tac*	*Eco*	*Tth*	PS3
Bst.	27.4	28.7	27.4	36.0	37.8	43.3	47.0	99.4 (Ref. *21*) 98.8 (Ref. *19*)

The values are expressed as percentages derived from Fig. 5. Abbreviations are: *Sce, S. cerevisiae* (*9*); *Kla, K. lactis* (*10*); *Spo, S. pombe* (*11*); *Ath, A. thaliana* (*12*); *Tac, T. acidophilum* (*26*); *Eco, E. coli* (*18*); *Tth, Thermus thermophilus* (*20*); PS3, thermophilic bacterium PS-3 (*19, 21*); and *Bst., Bacillus stearothermophilus.*

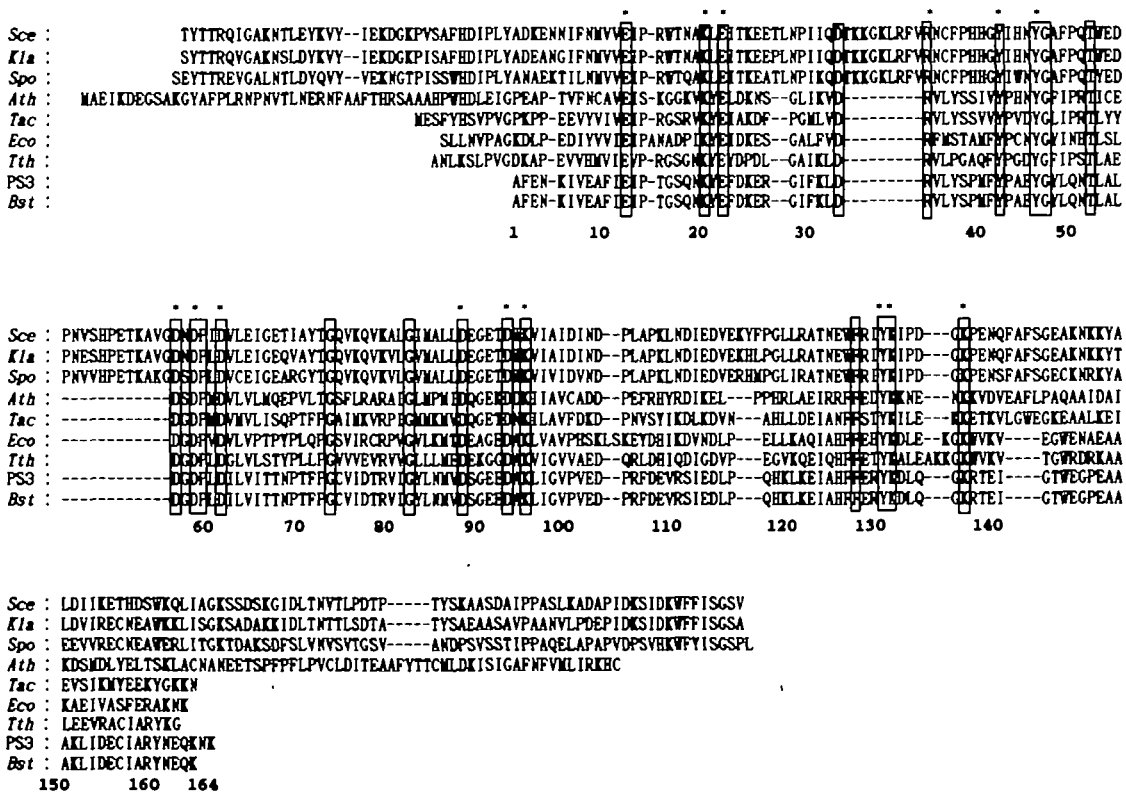

Fig. 5. **Alignment of the amino acid sequences of PPases from several sources.** The amino acid sequences of PPases from *S. cerevisiae* (*Sce*) (*9*), *K. lactis* (*Kla*) (*10*), *S. pombe* (*Spo*) (*11*), *A. thaliana* (*Ath*) (*12*), *T. acidophilum* (*Tac*) (*26*), *E. coli* (*Eco*) (*18*), *Thermus thermophilus* (*Tth.*) (*20*), thermophilic bacterium PS-3 (PS3) (*19*), and *Bacillus stearothermophilus* (*Bst.*) were aligned using the computer program GENETYX. Asterisks indicate the putative active site residues based on the tertiary structure of *Tth.* PPase (*23*). The boxed amino acids represent invariant residues among all PPases. The numbering of the residues is that of *Bst.* PPase.

residues are involved in the active-site cavity (*22*), and these residues are also conserved in *Bst.* PPase, namely, Glu12, Lys20, Glu22, Arg34, Tyr42, Tyr46, Asp56, Asp58, Asp61, Asp88, Asp93, Lys94, Tyr130, Lys131, and Lys136. In the case of *Tth.* PPase, eight other conserved residues might be of structural importance to the enzyme, such as being involved in β-barrel formation (*23*). It seems likely that eight other conserved residues are also responsible for structural integrity in *Bst.* PPase.

The Characteristics of Y46F and Y130F Variants—As described above, the three-dimensional structures and active sites of the *E. coli* and *Tth.* PPases have been determined at 1.9 and 2.0 Å, respectively (*22, 23*). Furthermore, in *E. coli* PPase, a site-directed mutagenesis study was performed with regard to the putative active site residues. It was reported that Tyr55 and Tyr141 in *E. coli* PPase form part of a hydrophobic cluster, and that the hydroxy groups of these tyrosines are crucial for catalysis and structural integrity (*28*). Therefore, on the basis of this information and the alignment of the primary structures of various PPases (Fig. 5), we focused on the two conserved Tyr residues in the *Bst.* PPase, Tyr46 and Tyr130 (corresponding to Tyr55 and Tyr141 in the *E. coli* PPase). To examine the contribution of the hydroxyl groups of these conserved tyrosines to the catalysis and thermostability of *Bst.* PPase, we constructed two variants, Y46F and Y130F, from which the hydroxyl group of a Tyr residue was eliminated. These variants were effectively expressed in *E. coli* cells. According to the purification procedure for the wild type enzyme, the two variants were purified to electrophoretically to homogeneity. Finally, we examined some of the characteristics of these variants. The specific activity of the wild type enzyme (recombinant *Bst.* PPase) was 687 units/mg, while Y46F and Y130F showed activities of 0.13 and 2.67 units/mg, respectively. The remarkable reduction in the specific activity of the two variants suggests that these tyrosine residues may be essential for enzyme activity. Furthermore, we investigated whether conformational changes may contribute to the reduction in specific activity. First, their circular dichroism (CD) spectra were measured in the far-UV region. The CD spectra showed secondary structures abundant in α-helix and β-sheet, and the mean residue ellipticity of each variant at 222 nm was almost the same as that of the wild type enzyme (Table II). Then, using the sole tryptophan (Trp143) as a probe, we explored the environment in the vicinity of Trp143 by measuring the fluorescence spectra as an indicator of conformational change. When excited at 295 nm, the emission spectra of the wild type and two variant enzymes showed almost no change in the maximum wavelength, as shown in Table II. This suggests that the gross reduction in the specific activity of Y46F and Y130F is not induced by drastic conformational changes.

Thermostability of Y46F and Y130F Variants—Next, we investigated the thermostability of Y46F and Y130F in the presence and absence of 1 mM Mg^{2+}, by measuring the CD spectra and fluorescence spectra after heating at high temperatures for 1 h. The CD spectra showed almost no differences in secondary structure between the wild type and two variants, either in the presence or absence of Mg^{2+}. On the other hand, the fluorescence spectra showed a red-shift effect of the maximum wavelength on the emission spectra as the temperature was raised. It has been reported that the maximum wavelength on the emission spectra is red-shifted as *Bst.* PPase is denatured because of

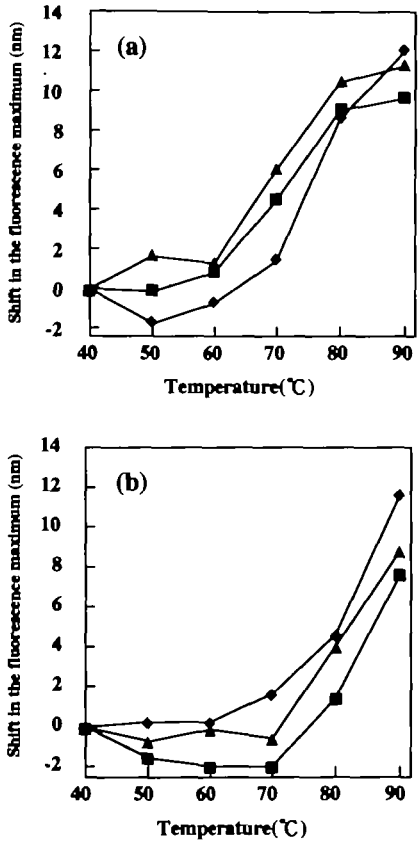

Fig. 6. **The shift in the fluorescence maxima of *Bst.* PPase and its variants at various temperatures.** The enzyme (0.1 mg/ml) was incubated in Tris-HCl buffer (pH 7.8) at various temperatures for 1 h and then the fluorescence spectra were measured at room temperature at an excitation wavelength of 295 nm. The maximum wavelength of the fluorescence spectrum was plotted as the relative shift compared to the spectrum at 40°C. (a) no Mg^{2+} addition; (b) in the presence of 1 mM Mg^{2+}. Symbols: ■, wild type; ▲, Y46F; ◆, Y130F.

TABLE II. **The characteristics of *Bst.* PPase and its variants, Y46F and Y130F.**

	Enzyme activity		Fluorescence and CD spectra		
	Specific activity (units/mg)	Relative activity[a] (%)	Max. WL[b] (nm)	Shift in WL[c] (nm)	$[\theta]_{222nm}$[d] (degree·cm²/dmol)
Bst. PPase (wild type)	687	100	333.8	0	−9,580
Y46F	0.13	0.02	334.6	+0.8	−8,340
Y130F	2.67	0.39	334.0	+0.2	−9,280

[a]The specific activity of *Bst.* PPase (wild type) was taken as 100%. [b]Max. WL means the maximum wavelength of the tryptophan fluorescence emission spectra. [c]Shift in WL means a shift in the maximum wavelength of the tryptophan fluorescence emission spectra. Wild type was taken as zero. [d]Values are the averaged values between 221.5 and 222.4 nm.

the hydrophilic environment around the sole fluorescence probe (Trp143) (*39*), and we utilized this result to evaluate the thermostability of the Tyr variants. In the absence of Mg^{2+}, Y46F showed a larger red shift than the wild type, while Y130F at first showed a small blue shift followed by a red shift above 70°C as shown in Fig. 6a. In the presence of 1 mM Mg^{2+} (Fig. 6b), the wild type enzyme exhibited a blue-shift effect after heating between 50 and 70°C, followed by a red shift above 80°C, whereas Y46F showed a slightly larger red shift than the wild type. Meanwhile, Y130F showed a similar red shift above 70°C as in the absence of Mg^{2+}, and there seemed to be no protection by the addition of Mg^{2+}. From these results, Y46F is slightly less stable than the wild type, although Mg^{2+}-induced thermostabilization was observed. On the other hand, Y130F seems to be more unstable than the wild type only in the presence of 1 mM Mg^{2+}. Thus, the data suggest that these two tyrosines are affected differently by Mg^{2+} and contribute to the thermostability of *Bst.* PPase in a distinct manner.

DISCUSSION

Proteins from thermophilic bacteria are generally thermostable, and the information about factors that contribute to the thermostability of proteins is thought to involve their amino acid sequences and can be obtained by comparing their sequences with those of mesophilic proteins. The *Bst.* PPase is a thermostable enzyme that is stabilized by the binding of divalent metal ions such as Mg^{2+} (*2*). Therefore, we determined the complete amino acid sequence of *Bst.* PPase by automated Edman degradation, as shown in Fig. 1, and compared it with those of PPases from procaryotes, eucaryotes, and archaebacteria. The *Bst.* PPase comprises 164 residues in a monomer with a calculated molecular mass of 18,796. As we previously reported (*2*), the molecular mass per subunit is estimated to be about 19 kDa by SDS-PAGE, which agrees well with the calculated molecular mass. Since the *Bst.* PPase has higher contents of Gly, Ile, Phe, Thr, Gln, Glu, and Arg residues than *E. coli* PPase, as shown in Table III, we can assume the possibility that these bulky amino acids may play a key role in the distinct characteristic differences between *E. coli* and *Bst.* PPases. However, in general, the amino acid composition of *Bst.* PPase is not so distinct from that of *E. coli* PPase (Table III). Therefore, an intricate conformational discrepancy may be a crucial factor for thermostability.

However, for our investigation of the relationship between function and structure, it is necessary to establish an overexpression system for the *Bst.* PPase gene in *E. coli* cells. Therefore, on the basis of the determined primary structure of *Bst.* PPase, we established an expression system for the *Bst.* PPase gene in *E. coli* cells using PCR. The deduced amino acid sequence from the base sequence of the *Bst.* PPase gene coincided completely with the determined primary structure at the protein level (Figs. 1 and 2). The codon usage of the gene, except for the primer region for PCR, indicates that it is highly similar to that of thermophilic bacteria PS-3 PPase (data not shown). Both *Bst.* and PS-3 are moderate thermophile and belong to the *Bacillus* genus, but the species of PS-3 was not identified and the bacteria may differ in their living environment [PS-3 was isolated from a hot spring (*40*); *Bst.* ATCC-12016 from flat sours in canned peas]. On the basis of the comparison between the two primary structures, *Bst.* is presumed to share a close evolutionary relationship with the thermophilic bacterium PS-3. As described above, the primary structure of PS-3 PPase is two amino acids longer than that of *Bst.* PPase at the C-terminus (*19*). However, the sequence of the *Bst.* enzyme is identical to that of the PS-3 enzyme (*21*) except for Pro70 at the amino acid level. Because the six bases coding these two amino acids correspond to the adjacent downstream region of the 3′-end primer, we could not confirm the reliability of this difference. The semi-synthetic gene was effectively expressed in *E. coli* JM109, and purification of the expressed enzyme to homogeneity was done electrophoretically. The estimated molecular weight of the recombinant *Bst.* PPase was the same as that of the authentic one as determined by SDS-PAGE. Furthermore, we examined the thermostability of the recombinant *Bst.* PPase and compared it with that of the recombinant *E. coli* PPase. As a result, the recombinant *Bst.* PPase appears more thermostable than the *E. coli* enzyme. Thus, we can utilize this expression system to investigate the structure-function relationship of *Bst.* PPase.

To investigate the role of the hydroxyl groups of the conserved Tyr residues in *Bst.* PPase, *i.e.* Tyr46 and Tyr130, we constructed two variants in which these tyrosine residues were replaced by phenylalanine (Y46F and Y130F). The specific activities of Y46F and Y130F were reduced to 0.02 and 0.39% of the wild type, respectively. This suggests that Tyr46 and Tyr130 in *Bst.* PPase must be crucial for enzyme activity. On the other hand, since their CD and fluorescence spectra were almost identical to those

TABLE III. **Comparison of amino acid compositions between *Bst.* and *E. coli* PPase.**

	Number of residues and their percentages	
	Bst. PPase (this study)	*E. coli* PPase (Ref. *18*)
Gly	11 (6.7%)	9 (5.1%)
Ala	10 (6.1)	16 (9.1)
Val	9 (5.5)	16 (9.1)
Leu	13 (7.9)	15 (8.6)
Ile	14 (8.5)	10 (5.7)
Met	2 (1.2)	3 (1.7)
Phe	9 (5.5)	6 (3.4)
Trp	1 (0.6)	2 (1.1)
Pro	10 (6.1)	13 (7.4)
Hpo[a]	79 (48.1%)	90 (51.4%)
Ser	4 (2.4%)	8 (4.6%)
Thr	8 (4.9)	4 (2.3)
Asn	6 (3.7)	7 (4.0)
Gln	5 (3.1)	2 (1.1)
Cys	2 (1.2)	2 (1.1)
Ntr[b]	25 (15.3%)	23 (13.1%)
Asp	13 (7.9%)	14 (8.0%)
Glu	18 (11.0)	15 (8.6)
Lys	11 (6.7)	16 (9.1)
His	2 (1.2)	5 (2.9)
Arg	8 (4.9)	4 (2.3)
Tyr	8 (4.9)	8 (4.6)
Hpi[c]	60 (36.6%)	62 (35.5%)
Total amino acid residues	164 (100%)	175 (100%)

[a]Hpo: Total number of hydrophobic amino acid residues. [b]Ntr: Total number of neutral amino acid residues. [c]Hpi: Total number of hydrophilic amino acid residues.

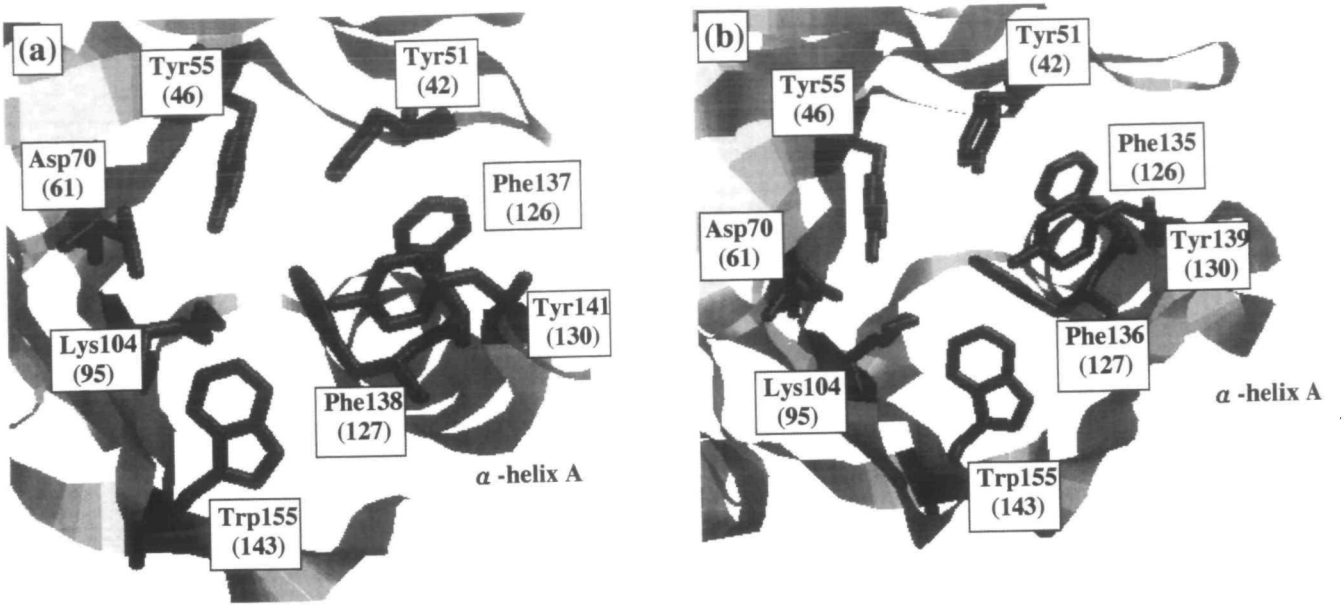

Fig. 7. **Three-dimensional structures of *E. coli* (a) and *Tth.* (b) PPases in the vicinity of the active site.** The three-dimensional structures of *E. coli* PPase (*41*) and *Tth.* PPase (*23*) were drawn by a Molecular Graphics Program, RasMol ver. 2.6, using coordinates from the X-ray crystal structure, 1faj and 2prd, respectively. The contours shown as thick lines indicate the side chains of each residue. The numbers in parentheses correspond to the amino acid number of *Bst.* PPase.

of the wild type, we confirmed no drastic conformational changes in these variants due to their substitutions. Next, we examined the thermostability of these variants in the presence and absence of Mg^{2+}. In a previous report (*2*), we suggested that Mg^{2+} can stabilize the conformation of *Bst.* PPase, and that its thermostability is then increased. From this viewpoint, we investigated the thermostability of the Tyr-substituted variants under the same conditions. As a result, compared with the wild type enzyme in the absence of Mg^{2+}, the thermostability of Y46F was slightly decreased, while Y130F was stabilized during heating below 70°C (Fig. 6a). In contrast, with the addition of 1 mM Mg^{2+}, the thermostability of Y46F was increased to the same level as the wild type, while no significant effect was seen for Y130F (Fig. 6b). This difference in Mg^{2+}-induced thermostability suggests that these variants have different Mg^{2+}-binding affinities. However, because the enzyme activities of the variants were very low (Y46F, 0.13 unit/mg; Y130F, 2.67 units/mg), accurate kinetic parameters are difficult to obtain. Additionally, based on the data of Native-PAGE, we estimated that the oligomeric structures of the two variants, Y46F and Y130F, were not changed by the substitutions (data not shown).

In the case of *E. coli* PPase, the relative activities of the corresponding variants, Y55F and Y141F, were reduced to 10 and 22% of the wild type (*28*). Moreover, the Y55F hexamer dissociated into trimers (*31*). From information on the three-dimensional structure of *E. coli* PPase, it appears that Tyr55 forms a hydrogen bond network with Asp70 and Lys104, and the phenyl ring of Tyr55 is in hydrophobic contact with the side chains of Tyr51 and Phe138 which, in turn, pack against Phe137 and Tyr141 (Fig. 7a). It was deduced that the destabilization of Y55F and Y141F are the result of disorder in these interactions (*28*). On the other hand, the corresponding variants for Y-PPase are Y93F and Y192F whose enzyme activities are reduced to 3 and 20% of the wild type activity, respectively. However, no drastic changes in thermostability or oligomeric structure were observed in these variants (*32*). The reason for this may be that Y-PPase is a dimeric enzyme, whereas *E. coli* PPase is hexameric, and *E. coli* PPase consists of two trimers with the trimer-trimer interface formed by an α-helix A containing Phe137, Phe138, and Tyr141 (Fig. 7a) (*28*). In contrast, the corresponding α-helix in Y-PPase is not involved in the dimeric contact region (*29*). Since the substituted Tyr residues (Tyr55/Tyr141 in *E. coli* PPase, Tyr93/Tyr192 in Y-PPase) are located in different environments in each PPase, we conclude that these substituted variants exhibit the different effects. It was also found from the X-ray data that the role of the corresponding tyrosines in *Tth.* PPase is very similar (*23*). The bottom of the active-site cavity is formed by a cluster of aromatic amino acids that includes Tyr51, Pro52, Tyr55, Phe135, Phe136, and Tyr139 (Fig. 7b). The three tyrosines point their hydroxyl groups toward the active-center. However, it is difficult to foresee the effect of removing a hydroxyl group by substitution, *i.e.* variants Y51F, Y55F, and Y139F. In this respect, studies on the role of tyrosine residues are now underway, using the *Tth.* PPase gene expression system in *E. coli* (*20*).

On the other hand, although the three-dimensional structure of *Bst.* PPase has not yet been determined, the corresponding residues, including Tyr46 and Tyr130, are also highly conserved in *Bst.* PPase (Fig. 5). Therefore, we can infer that the active site of *Bst.* PPase may be formed from the similar residues, *i.e.* Tyr42, Tyr46, Asp61, Lys95, Phe126, Phe127, and Tyr130 (Fig. 7, a and b), and interactions as in the *E. coli* and *Tth.* enzymes, and these may then be responsible for PP_i hydrolysis. In this study, we suggest critical contributions of Tyr46 and Tyr130 to enzyme activity, but show that the secondary structure and the environment around the sole tryptophan residue

(Trp143) are unaltered by tyrosine substitution, as described above. Nevertheless, the thermostabilities of these variants differ as shown in Fig. 6, a and b. Thus, we point out that some interactions around Tyr46 and Tyr130 are perturbed in different manners, which then affect the environment in the vicinity of Trp143 after heating, as shown in Fig. 7, a and b. Although further investigations are needed, it appears that Tyr46 and Tyr130 may be essential for the enzyme activity and structural integrity of the active site of *Bst.* PPase.

We thank Ishikawajima-Harima Heavy Industries for providing a research grant, and S. Kawai, M. Hikita, K. Sugiyama, K. Nemoto, H. Miyagawa, M. Korenaga, and M. Ikeda-Kawai for their technical assistance. Our thanks are also due to T. Sakamoto, M. Takanashi, T. Minami, J. Takeda, S. Ariga, M. Hattori, M. Ono, M. Onodera, and H. Narita for their technical contributions, as well as K. Shibuya, M. Watanabe, Y. Takahashi, and J. Shigeta for helpful discussion.

REFERENCES

1. Lahti, R. (1983) Microbial inorganic pyrophosphatases. *Microbiol. Rev.* **47**, 169-179
2. Hachimori, A., Shiroya, Y., Hirato, A., Miyahara, T., and Samejima, T. (1979) Effects of divalent cations on thermophilic inorganic pyrophosphatase. *J. Biochem.* **86**, 121-130
3. Lahti, R. and Niemi, T. (1981) Purification and some properties of inorganic pyrophosphatase from *Streptococcus faecalis*. *J. Biochem.* **90**, 79-85
4. Obmolova, G., Kuranova, I., and Teplyakov, A. (1993) Purification, crystallization and preliminary X-ray analysis of inorganic pyrophosphatase from *Thermus thermophilus*. *J. Mol. Biol.* **232**, 312-313
5. Yang, Z. and Wensel, T.G. (1992) Inorganic pyrophosphatase from bovine retinal rod outer segments. *J. Biol. Chem.* **267**, 24634-24640
6. Hachimori, A., Fujii, T., Ohki, K., and Iizuka, E. (1983) Purification and properties of inorganic pyrophosphatase from porcine brain. *J. Biochem.* **93**, 257-264
7. Meyer, W. and Schäfer, G. (1992) Characterization and purification of a membrane-bound archaebacterial pyrophosphatase from *Sulfolobus acidocaldarius*. *Eur. J. Biochem.* **207**, 741-746
8. Richter, O.M.H. and Schäfer, G. (1992) Purification and enzymic characterization of the cytoplasmic pyrophosphatase from the thermoacidophilic archaebacterium *Thermoplasma acidophilum*. *Eur. J. Biochem.* **209**, 343-349
9. Cohen, S.A., Sterner, R., Keim, P.S., and Heinrikson, R.L. (1978) Covalent structural analysis of yeast inorganic pyrophosphatase. *J. Biol. Chem.* **253**, 889-897
10. Stark, M.R. and Milner, J.S. (1989) Cloning and analysis of the *Kluyveromyces lactis* TRP1 gene: a chromosomal locus flanked by genes encoding inorganic pyrophosphatase and histone H3. *Yeast* **5**, 35-50
11. Kawasaki, I., Adachi, N., and Ikeda, H. (1990) Nucleotide sequence of *S. pombe* inorganic pyrophosphatase. *Nucleic Acids Res.* **18**, 5888
12. Kieber, J.J. and Signer, E.R. (1991) Cloning and characterization of an inorganic pyrophosphatase gene from *Arabidopsis thaliana*. *Plant Mol. Biol.* **16**, 345-348
13. Yang, Z. and Wensel, T.G. (1992) Molecular cloning and functional expression of cDNA encoding mammalian inorganic pyrophosphatase. *J. Biol. Chem.* **267**, 24641-24647
14. Kolakowski Jr., L.F., Schloesser, M., and Cooperman, S. (1988) Cloning, molecular characterization and chromosome localization of the inorganic pyrophosphatase (PPA) gene from *S. cerevisiae*. *Nucleic Acids Res.* **16**, 10441-10452
15. Lundin, M., Baltscheffsky, H., and Ronne, H. (1991) Yeast PPA2 gene encodes a mitochondrial inorganic pyrophosphatase that is essential for mitochondrial function. *J. Biol. Chem.* **266**, 12168-12172
16. Kuranova, S.A., Vorobjeva, N.N., Nazarova, T.I., and Avaeva, S.M. (1993) Expression of *Saccharomyces cerevisiae* inorganic pyrophosphatase in *Escherichia coli*. *FEBS Lett.* **333**, 280-282
17. Heikinheimo, P., Lehtonen, J., Baykov, A., Lahti, R., Cooperman, B.S., and Golderman, A. (1996) The structural basis for pyrophosphatase catalysis. *Structure* **4**, 1491-1508
18. Lahti, R., Pitkäranta, T., Valve, E., Ilta, I., Kukko-Kalske, E., and Heinonen, J. (1988) Cloning and characterization of the gene encoding inorganic pyrophosphatase of *Escherichia coli* K-12. *J. Bacteriol.* **170**, 5901-5907
19. Maruyama, S., Maeshima, M., Nishimura, M., Aoki, M., Ichiba, T., Sekiguchi, J., and Hachimori, A. (1996) Cloning and expression of the inorganic pyrophosphatase gene from thermophilic bacterium PS-3. *Biochem. Mol. Biol. Int.* **40**, 679-688
20. Satoh, T., Samejima, T., Watanabe, M., Nogi, S., Takahashi, Y., Kaji, H., Teplyakov, A., Obmolova, G., Kuranova, I., and Ishii, K. (1998) Molecular cloning, expression and site-directed mutagenesis of inorganic pyrophosphatase from *Thermus thermophilus* HB8. *J. Biochem.* **124**, 79-88
21. Ichiba, T., Takenaka, O., Samejima, T., and Hachimori, A. (1990) Primary structure of the inorganic pyrophosphatase from thermophilic bacterium PS-3. *J. Biochem.* **108**, 572-578
22. Harutyunyan, E.H., Oganessyan, V.Y., Oganessyan, N.N., Avaeva, S.M., Nazarova, T.I., Vorobyeva, N.N., Kurilova, S.A., Huber, R., and Mather, T. (1997) Crystal structure of holo inorganic pyrophosphatase from *Escherichia coli* at 1.9 Å resolution. Mechanism of hydrolysis. *Biochemistry* **36**, 7754-7760
23. Teplyakov, A., Obmolova, G., Wilson, K.S., Ishii, K., Kaji, H., Samejima, T., and Kuranova, I. (1994) Crystal structure of inorganic pyrophosphatase from *Thermus thermophilus*. *Protein Sci.* **3**, 1098-1107
24. Salminen, T., Teplyakov, A., Kankare, J., Cooperman, B.S., Lahti, R., and Goldman, A. (1996) An unusual route to thermostability disclosed by the comparison of *Thermus thermophilus* and *Escherichia coli* inorganic pyrophosphatases. *Protein Sci.* **5**, 1014-1025
25. Meyer, W., Moll, R., Kath, T., and Schäfer, G. (1995) Purification, cloning, and sequencing of archaebacterial pyrophosphatase from the extreme thermoacidophile *Sulfolobus acidocaldarius*. *Arch. Biochem. Biophys.* **319**, 149-156
26. Richter, O.M.H. and Schäfer, G. (1992) Cloning and sequencing of the gene for the cytoplasmic inorganic pyrophosphatase from the thermoacidophilic archaebacterium *Thermoplasma acidophilum*. *Eur. J. Biochem.* **209**, 351-355
27. Kankare, J., Salminen, T., Lahti, R., Cooperman, B.S., Baykov, A.A., and Goldman, A. (1996) Crystallographic identification of metal-binding sites in *Escherichia coli* inorganic pyrophosphatase. *Biochemistry* **35**, 4670-4677
28. Salminen, T., Käpylä, J., Heikinheimo, P., Kankare, J., Goldman, A., Heinonen, J., Baykov, A.A., Cooperman, B.S., and Lahti, R. (1995) Structure and function analysis of *Escherichia coli* inorganic pyrophosphatase: Is a hydroxide ion the key to catalysis? *Biochemistry* **34**, 782-791
29. Harutyunyan, E.H., Kuranova, I.P., Vainshtein, B.K., Höhne, W.E., Lamzin, V.S., Dauter, Z., Teplyakov, A.V., and Wilson, K.S. (1996) X-ray structure of yeast inorganic pyrophosphatase complexed with manganese and phosphate. *Eur. J. Biochem.* **239**, 220-228
30. Avaeva, S.M., Rodina, E.V., Kurilova, S.A., Nazarova, T.I., Vorobyeva, N.N., Harutyunyan, E.H., and Oganessyan, V.Y. (1995) Mg^{2+} activation of *Escherichia coli* inorganic pyrophosphatase. *FEBS Lett.* **377**, 44-46
31. Fabrichniy, I.P., Kasho, V.N., Hyytiä, T., Salminen, T., Halonen, P., Dudarenkov, V.Y., Heikinheimo, P., Chernyak, V.Y., Goldman, A., Lahti, R., Cooperman, B.S., and Baykov, A.A. (1997) Structural and functional consequences of substitutions at the tyrosine 55-lysine 104 hydrogen bond in *Escherichia coli* inorganic pyrophosphatase. *Biochemistry* **36**, 7746-7753
32. Pohjanjoki, P., Lahti, R., Goldman, A., and Cooperman, B.S. (1998) Evolutionary conservation of enzymatic catalysis: Quantitative comparison of the effects of mutation of aligned residues in *Saccharomyces cerevisiae* and *Escherichia coli* inorganic pyro-

phosphatase on enzymatic activity. *Biochemistry* **37**, 1754-1761
33. Hachimori, A., Takeda, A., Kaibuchi, M., Ohkawara, N., and Samejima, T. (1975) Purification and characterization of inorganic pyrophosphatase from *Bacillus stearothermophilus*. *J. Biochem.* **77**, 1177-1183
34. Saito, H. and Miura, K. (1963) Preparation of transforming deoxyribonucleic acid by phenol treatment. *Biochim. Biophys. Acta* **72**, 619-629
35. Kaji, H., Kumagai, I., Takeda, A., Miura, K., and Samejima, T. (1990) Studies on chemical synthesis of human cystatin A gene and its expression in *Escherichia coli*. *J. Biochem.* **105**, 143-147
36. Peel, J.L. and Loughman, B.C. (1957) Some observations on the role of copper ions in the reduction of phosphomolybdate by ascorbic acid and their application in the determination of inorganic orthophosphate. *Biochem. J.* **65**, 709-716
37. Lowry, O.H., Rosebrough, N.J., Farr, A.L., and Randall, R.J. (1951) Protein measurement with the Folin phenol reagent. *J. Mol. Chem.* **193**, 265-275
38. Shiroya, Y. and Samejima, T. (1985) The specific modification of histidyl residues of inorganic pyrophosphatase from *Bacillus stearothermophilus* by photooxidation. *J. Biochem.* **98**, 333-339
39. Sola, M.P., Ferreira, A.P., Lemos, A.P., and Meyer, F. (1997) Carbohydrate protection of enzyme structure and function against guanidium chloride treatment depends on the nature of carbohydrate and enzyme. *Eur. J. Biochem.* **248**, 24-29
40. Yoshida, M., Sone, N., Hirata, H., and Kagawa, Y. (1975) A highly stable adenosine triphosphatase from a thermophilic bacterium. *J. Biol. Chem.* **250**, 7910-7916
41. Kankare, J., Salminen, T., Lahti, R., Cooperman, B.S., Baykov, A.A., and Goldman, A. (1996) Structure of *Escherichia coli* inorganic pyrophosphatase at 2.2 Å resolution. *Acta Cryst.* **D52**, 551-563